European Journal of Radiology 113 (2019) 7–14

Contents lists available at ScienceDirect

European Journal of Radiology

journal homepage: www.elsevier.com/locate/ejrad

Research article

MR features based on LI-RADS identify cytokeratin 19 status of hepatocellular carcinomas

Xin-Xing Hu[a], Wen-Tao Wang[a], Li Yang[a], Zhao-Xia Yang[a], He-Yue Liang[a], Ying Ding[a], Yuan Ji[b], Meng-Su Zeng[a], Sheng-Xiang Rao[a,*]

[a] Department of Radiology, Zhongshan Hospital, Fudan University, and Shanghai Medical Imaging Institute, Shanghai, China
[b] Department of Pathology, Zhongshan hospital, Fudan University, Shanghai, China

ARTICLE INFO

Keywords:
Hepatocellular carcinoma
Magnetic resonance imaging
Cytokeratin 19

ABSTRACT

Objective: To retrospectively evaluate the value of MR features based on Liver Imaging Reporting and Data System (LI-RADS ver.2017) for identifying the status of cytokeratin (CK) 19 expression of HCC before surgery.
Methods: A total of 201 patients with 207 HCCs who underwent MR imaging were reviewed retrospectively. MR features based on LI-RADS ver.2017 as well as clinical data were compared between CK19-positive (n = 51) and CK19-negative (n = 156) HCCs groups. Potential predictive parameters were identified by univariate and multivariate logistic regression analysis and diagnostic odds ratios (ORs) were recorded.
Results: MR features including targetoid appearance (p = 0.001) was more frequently observed while non-peripheral "washout" (p < 0.0001) and non-rim arterial phase hyper-enhancement (p < 0.0001) were found less frequently in CK19-positive HCCs compared to CK19-negative HCCs. At multivariate analysis, serum alphafetoprotein (AFP) > 20 ng/ml (OR = 5.9) and targetoid appearance (OR = 4.2) and non-peripheral "washout" (OR = 0.2) were significant independent predictors of CK19-positive HCCs.
Conclusion: Targetoid appearance and absence non-peripheral "washout" combined with elevated AFP were useful for differentiating CK19-positive HCCs from CK19-negative HCC.

1. Introduction

Liver cancer is the second most frequent cause of cancer death worldwide [1,2]. A total of 70%–90% primary liver cancers occurring are hepatocellular carcinoma (HCC) in the world and recently HCC is increasing in incidence in many countries [2,3]. Most often, HCC represents a multistep process on a background of chronic hepatitis or cirrhosis [4–6].

Cytokeratin 19 (CK19), a marker of progenitor cell, has currently been identified as a marker for the biliary-type. It expresses in several types of human cancers, including papillary thyroid carcinoma, breast cancer, lung cancer, intrahepatic cholangiocarcinoma, and recently HCC, but it is not expressed in normal hepatocytes [7–9]. In prior studies, significant findings had elucidated that HCC with CK19 expression was related to the adverse clinicopathologic outcomes, such as tumor aggressiveness, vascular invasion, tumor recurrence and poor prognosis compared to HCC without CK19 expression [7,10,11] which may be predominantly attributed to the different origins of hepatocytes. In the clinical practice, CK19 protein expression is tested by immunohistochemistry after performing invasive procedures such as surgical resection or biopsy. Therefore, it is necessary to develop a non-invasive alternative approach to assess the expression of CK19 of HCC.

Cross-sectional imaging modality such as computed tomography (CT) or magnetic resonance (MR) imaging is routinely performed as a noninvasive tool for surveillance [12,13] and characterization of focal liver lesions [14,15]. Furthermore, contrast-enhanced MR imaging is currently regarded as one of the best techniques in the diagnosis of HCC due to different MR sequences information it can provide [15]. Lesions in patients at risk of HCC can be categorized based on LI-RADS v2017 using major features: nonrim arterial phase hyperenhancement (APHE),

Abbreviations: MR, magnetic resonance; LI-RADS, Liver Imaging Reporting and Data System; CK19, cytokeratin 19; HCC, hepatocellular carcinoma; ORs, odds ratios; AFP, alphafetoprotein; CT, computed tomography; APHE, arterial phase hyper-enhancement; VIBE, volumetric interpolated breath-hold examination; PACS, picture archiving and communication system; CI, confidence interval; CA-199, carbohydrate antigen-199; CEA, carcino embryonie antigen; TB, total bilirubin level; MVI, microvascular invasion; ICC, intrahepaticcholangiocarcinom; DWI, diffusion weighted images

* Corresponding author at: Department of Radiology, Zhongshan Hospital, Fudan University, and Shanghai Medical Imaging Institute, 180 Fenglin Rd., 200032, Shanghai, China.
E-mail address: raoxray@163.com (S.-X. Rao).

https://doi.org/10.1016/j.ejrad.2019.01.036
Received 1 October 2018; Received in revised form 18 January 2019; Accepted 30 January 2019

nonperipheral "washout", enhancing "capsule", threshold growth and size. Additionally, targetoid appearance is a criterion for LR-M (probably or definitely malignant, not HCC specific). [14,15] Compared to typical CK19-negative HCCs, CK19-positive HCC has more biologically invasive characteristics which may have some imaging appearances associated with high aggressiveness of tumor. Studies demonstrated that some MR imaging features had potential value for indicating HCC expressing CK19 [16–18], such as hypovascularity on arterial phase [18] (related to worse histological grades [19]) or arterial phase irregular rim enhancement [16] (potential biomarker for microvascular invasion of HCC [20]), etc. We should explore the usefulness of MR imaging features for recognizing the CK19 expressions in HCC lesions. Therefore, the purpose of this study aimed to determine whether major and LR-M MR features based on LI-RADS ver.2017 of HCC can aid in assessing the status of CK19 expression of HCC before surgery.

2. Materials and methods

2.1. Study patients

The protocol for this retrospective study was approved by the Institutional Review Board of XXX with waiver of informed consent. A total of 216 consecutive HCC patients were first identified from April 2015 to February 2016 in our hospital. Eligible patients were included according to the following criteria: (1) performing preoperative contrast enhancement MR imaging; (2) pathologically proven HCC after hepatectomy or liver transplantation, and (3) availability of immunohistochemical marker of CK19 from pathology. Patients were excluded if (1) patients underwent curative therapy (transplantation, resection, ablation, embolization or others) prior to MR imaging (n = 5);(2) patients had history of other malignant tumors(n = 2);(3) important clinical data[such as alphafetoprotein (AFP), carbohydrate antigen-199(CA-199),carcino embryonie antigen(CEA),total bilirubin level (TB), albumin, platelet etc.)]. cannot be available (n = 8).Finally, 201 HCC patients with 207 lesions were enrolled for analysis on the basis of CK19 marker (Fig. 1).Patient characteristics including radiological, clinical and pathologic data were evaluated by univariate and multivariate Analysis.

2.2. Imaging acquisition

All MRI abdominal examinations were performed on 1.5 or 3.0 T clinical scanner (Magnetom Avanto/Verio; Siemens Healthcare, Erlangen, Germany)using a body phased-array coil and a spine array coil. The standard imaging protocol consisted of T2-weighted, T1-weighted (in-phase and out-of-phase), diffusion-weighted (b = 0, 500 s/mm^2), and 3D gradient echo sequence with volumetric interpolated breath-hold examination (VIBE) (GRAPPA (R = 2)) was performed before and after injection of contrast media. The gadopentetate dimeglumine (Magnevist; Bayer Healthcare, Germany, 0.1 mmol/kg) was injected at a rate of 2 ml/s followed by a maximum dose of 20-mL saline flush. Hepatic arterial, portal, and equilibrium phase images were obtained respectively at 20–30 s, 60–90 s, and 180 s after contrast medium injection. The MR scan parameters refer to Table 1.

2.3. Imaging analysis

All the MR images were reviewed using a picture archiving and communication system (PACS; Pathspeed, GE Medical Systems Integrated Imaging Solutions, Prospect, IL, USA).Two abdominal radiologists (XXX and XXX with 16 years and 3 years of experience, respectively) who were blinded to the pathological results assessed the MR features by consensus.At first, both of the observers were provided a detailed same instruction before the evaluation of this study based on the LI-RADS ver.2017[15], which demonstrated a standardized explanation of terminology and criteria for interpretation and reporting of liver observations. And then for training purposes, the two observers were provided 15 patients MR images in a format identical to the study patient

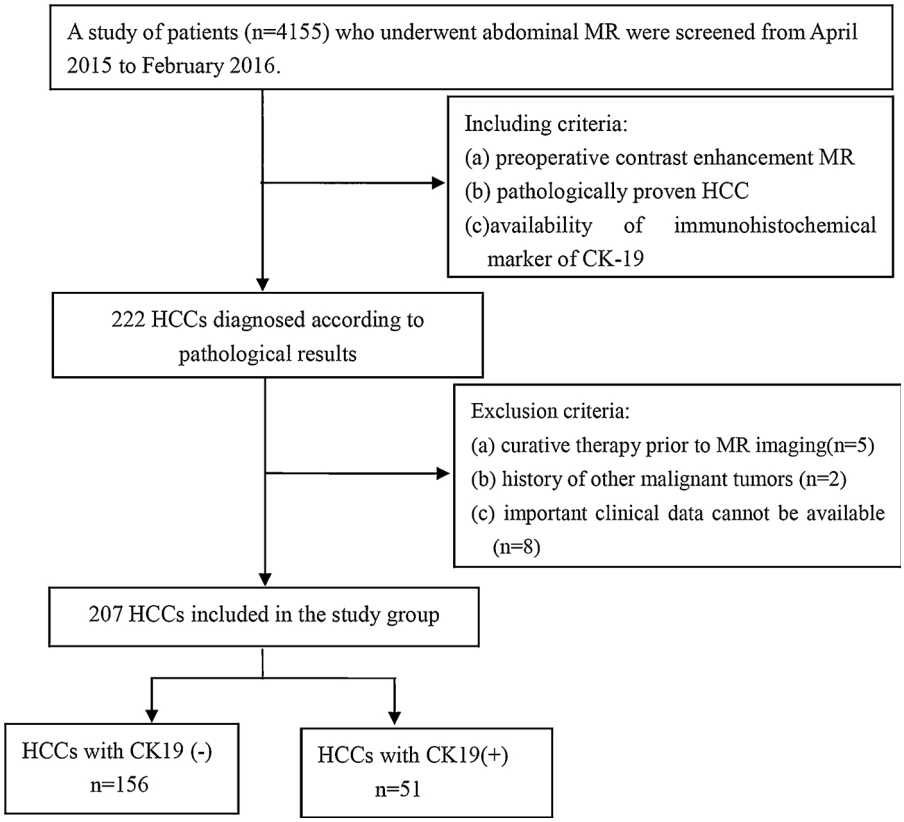

Fig. 1. Flowchart shows inclusion and exclusion criteria.

Table 1
Scan Sequences and Parameter of MR System.

Verio 3.0 T					Avanto 1.5T	
Parameter	TSE T2WI	DWI	3D-VIBE	T1WI (in/out of phase)	TSE T2WI	DWI
TR (ms)	3000	3400	4.1	195	3300	2400 ~ 2600
TE (ms)	83	70	1.4	2.31/3.69	70	66
NEX	1	1	1	1	1	1
Matrix	165 × 320	128 × 80	200 × 352	180 × 320	207 × 384	112 × 128
FOV(mm2)	285 × 214 ~ 285 × 380	285 × 214 ~ 285 × 380	285 × 214 ~ 285 × 380	285 × 214 ~ 285 × 380	330 × 330 ~ 380 × 380	330 × 330 ~ 380 × 380
Inversion angle	140°	/	9°	70°	150°	/
Slice thickness (mm)	5.5	6	3	5	7	7
Slice gap (mm)	1.1	1.8	0	1	2.1	2.1

Verio 3.0 T	Avanto 1.5T	Area 1.5T			
Parameter	T1WI (in/out of phase)	TSE T2WI	DWI	3D-VIBE)	T1WI (in/out of phase)
TR (ms)	118	3500	3200	4.38	6.87
TE (ms)	2.05/5.04	84	56	1.93	2.38/4.76
NEX	1	1	1	1	1
Matrix	144 × 256	194 × 256	84 × 128	216 × 288	180 × 256
FOV(mm2)	330 × 330 ~ 380 × 380	360 × 360	380 ~ 400 × 300 ~ 324	380 ~ 400 × 300 ~ 324	330 × 330 ~ 380 × 380
Inversion angle	70°	140°	/	12	70°
Slice thickness (mm)	7	8	5.5	5	7
Slice gap (mm)	2.1	2	2	0	2

Note;MR,magnetic resonance;TSE,turbo spin echo;T2WI,T2-weighted imaging;DWI,diffusion-weighted imaging;GRE,gradient echo; T1WI:T1-weighted imaging;3D VIBE,three dimension volumetric interpolated breath-hold examination;TR,repetition time;TE,echo time;NEX,number of excitation;FOV,field of view.

Table 2
Patients baseline Characteristics.

Variable	All	K-19		P-value
		Positive	Negative	
No. Of patients	201	51(25.4%)	150(74.6%)	
No. Of lesions	207	51(24.6%)	156(75.4%)	
Sex(Male/female)	170(84.6%)/31(15.4%)	39(76.5%)/12(23.5%)	131(87.3%)/19(12.7%)	0.064
Age(years)	55.9 ± 11.1	55.1 ± 11.9	56.2 ± 10.8	0.55
Maximum diameter of tumor (mm)	53.4 ± 87.7	54.3 ± 35.6	53.1 ± 34.0	0.838
AFP > 20 ng/ml (Yes/no),	123(59.4%)/84(40.6%)	43(84.3%)/8(15.7%)	80(51.3%)/76(48.7%)	< **0.0001**
CA-199 > 37U/ml (Yes/no),	36(17.4%)/171(82.6%)	12(23.5%)/39(76.5%)	24(15.45)/132(84.6%)	0.183
CEA > 5 ng/ml (Yes/no),	23(11.1%)/184(88.9%)	8(15.7%)/43(84.3%)	15(9.6%)/141(90.4%)	0.231
TB(μmol/L),	14.7 ± 13.9	13.6 ± 8.0	15.1 ± 15.4	0.501
Albumin (g/L),	41.0 ± 6.4	40.0 ± 9.3	41.3 ± 5.2	0.212
Platelet (1×10^9/L),	168.2 ± 72.7	169.0 ± 84.3	168.0 ± 68.8	0.588
HBV/HCV/No*,	164(79.2%)/9(4.3%)/34(16.5%)	37(72.5%)/5(9.8%)/9(17.7%)	127(81.4%)/4(2.6%)/25(16%)	0.079
portal vein thrombosis (Yes/no)	15(7.2%)/192(92.8%)	3(5.9%)/48(94.1%)	12(7.7%)/144(92.3%)	0.903
MVI(Yes/no)	89(43.%)/118(57%)	26(51%)/25(49%)	63(40.4%)/93(59.6%)	0.186

Note: AFP, alphafetoprotein; CA-199, carbohydrate antigen19-9; CEA, carcino embryonie antigen; TB, total bilirubin; HBV, hepatitis B varus; HCV, hepatitis C varus; MVI, microvascular invasion.
No* stands for no HBV and HCV infection.

images so as to practice before evaluation of the study. Besides that, the practice patients were not included in our patients study. The readers were also told that the patients had HCC tumors without any other knowledge of illness history, laboratory examination and pathological findings. The above-mentioned measures were taken to minimize the effects, achieve optimal results and avoid the training bias in our study.

We evaluated the morphological features based on the LI-RADS ver.2017 diagnostic algorithm, which included major imaging features and LR-M criteria as follows: non-rim APHE, non-peripheral washout, enhancing “capsule”, targetoid appearance on DWI or contrast-enhanced images(rim APHE, peripheral "washout", delayed central enhancement), as well as other imaging features including mild-moderate T2 hyperintensity, restricted diffusion, corona enhancement, as well as tumor margin, tumor morphologic features (including round or oval, round or oval with focal protrusions, lobulated and irregularlesions which are unable to be classified).

2.4. Histological diagnosis

Surgically resected HCC specimens were 10% formalin solution fixed and paraffin embedded in all patients. Immunohistochemical staining was carried out for CK19. The monoclonal antibodies against CK19 (1:200 dilution, BA17, GeneTax, San Antonio, TX, USA) were utilized. Immunoreactivity was evaluated as a positive per cent area for CK19 marker. In addition, the pathologist who was blind to patient’s imaging features determined the percentage of positive cells. CK19 positivity was defined as membranous and/or cytoplasmic expression in ≥5% of tumor cells with moderate or strong intensity. In our study, we classified HCC into “CK19-positive group (CK19 marker≥5%)” and “CK19-negative group (CK19 < 5%).

2.5. Statistical analysis

Continuous variables were compared using the Student’s *t*-test or Mann-Whitney U test, where appropriate. Categorical variables were compared using Pearson’s chi-squared test or Fisher’s exact test. First, univariable logistic regression analysis was performed to identify which of the patients’ history, laboratory, final pathological results and patients’ MR imaging data could be helpful to discriminate between CK19 positive /negative group as the dependent outcome. Subsequently, variables with P < 0.05 in univariate analysis were entered into multiple logistic regression analysis to identify significant independent risk factors with the odds ratio (OR) as well as 95% confidence interval (CI). Backward was performed:all variables were chosen to enter the multivariate analyses at once, then the variable which had the maximum value of P-value was eliminated each time until all variables are significant.Values of P < 0.05 by the two-tailed test were considered statistically significant. All date analyses were performed using IBM SPSS software (ver 20.0. SPSS, Chicago, IL).

3. Results

3.1. Patient sample

The HCC with CK19 positive group was comprised of 51 patients (39 men,12 women; median age, 54 years; range, 30–75 years) and CK19 negative HCC group was consisted of 150 patients (131 men,19 women; median age,57.5 years; range, 25–79 years). And the p values comparing sex and age distributions between the groups was 0.064 and 0.05,respectively. The serumAFP level was significantly higher in the CK19 positive group(mean ± standard deviation = 5121.8 ± 9838.1) than in the CK19 negative group(mean ± standard deviation = 2315.8 ± 8185.8) (p < 0.0001). The median and interquartile ranges in CK19 positive group(median = 291.45, interquartile ranges = 3001.55)were respectively higher than in CK19 negative group (median = 22.5, interquartile ranges = 221.15)(p < 0.001).AFP levels higher than 20 ng/ml were observed in 43/51(84.3%) HCC lesions in CK19 positive group and 80/156(51.3%) in CK19 negative group (p < 0.0001), respectively. The CA -199 level was higher than 37U/ml in 17.4% of HCC lesions (36/207) and CEA levels was higher than 5 ng/ml in 11.1% of HCC lesions (23/207). Age, sex, maximum diameter of tumor, CA-199,CEA, TB,platelet count, albumin, disease origin (hepatitis B/C or no), portal vein thrombosis and microvascular invasion (MVI) did not show significant difference between the CK19 positive HCCs group and CK19 negative HCCs group. The main patients characteristics are shown in Table 2.

3.2. MRI findings

3.2.1. MR signal characteristics

Upon dynamic enhancement pattern, non-rim APHE was more common in CK19 negative HCCs group(118/156, 75.6%) than it wasin

Table 3
MR Features of HCC.

Variable	K-19(+)	K-19(-)	P-value
Signal on T_2-weighted images			0.588
①hyperintense	49(96.1%)	146(93.6%)	
②isointense	0(0%)	5(3.2%)	
③hypointense	2(3.9%)	5(3.2%)	
Signal on T_1-weighted images			0.474
①hyperintense	0(0%)	5(3.2%)	
②isointense	0(0%)	2(1.3%)	
③hypointense	51(100%)	149(95.5%)	
Signal on DWI images			0.503
①hyperintense	50(98.0%)	145(92.9%)	
②isointense	1(2.0%)	6(3.8%)	
③hypointense	0(0%)	5(3.3%)	
nonrim APHE (yes/no)	22(43.1%)/29(56.9%)	118(75.6%)/38(24.4%)	< **0.0001**
nonperipheral "washout" (yes /no)	16(31.4%)/35(68.6%)	109(69.9%)/47(30.1%)	< **0.0001**
Hemorrhage(Yes/no)	13(25.5%)/38(74.5%)	44(28.2%)/112(71.8%)	0.706
Fat content(Yes/no)	12(23.5%)/39(76.5%)	32(20.5%)/124(79.5%)	0.648
enhancing "capsule"(Yes/no)	49(96.1%)/2(3.9%)	156(100%)/0(0%)	0.06
Corona enhancement(Yes/no)	2(3.9%)/49(96.1%)	2(1.3%)/154(98.7%)	0.547
Cholangiectasis (Yes/no)	2(3.9%)/49(96.1%)	3(1.9%)/153(98.1%)	0.778
Targetoid appearance (Yes/no)	11(21.6%)/40(78.4%)	9(5.8%)/147(94.2%)	**0.001**
Liver surface invasion(Yes/no)	21(41.2%)/30(58.8%)	42(26.9%)/114(73.1%)	0.055
Tumor margin(smooth/no)	32(62.7%)/16(37.3%)	116(74.4%)/40(25.6%)	0.296
MR gross morphology			**0.003**
①round or oval	28(54.9%)	115(73.7%)	
②round or oval with focal protrusiongs	8(15.7%)	16(10.3%)	
③lobulated	12(23.5%)	10(6.4%)	
④irregular with clear margin or blurred with fuzzy edge	3(5.9%)	15(9.6%)	

Note: MR,magnetic resonance; HCC,hepatocellular carcinoma; DWI,diffusion weighted imaging; APHE: arterial phase hyperenhancement ; Cholangiectasis presented that intrahepatic bile duct diameter is greater than 4mm ; Liver surface invasion presented that when the lesion is adjacent to the surface of the liver, the liver capsule is invaded.

CK19 positive HCCs group(22/51, 43.1%) ($p < 0.0001$). There were no lesions without APHE in CK19 positive HCCs group and CK19 negative HCCs group. It is obvious that about 57%(29/51) of CK19 positive HCCs and 24% (38/156) of CK19 negative HCCs had rim APHE. And non-peripheral washout was more observed in CK19 negative HCCs group(109/156, 69.9%) than it was in CK19 positive HCCs group (16/51,31.4%) ($p < 0.0001$), while enhancing capsule showed no significant difference between the two groups ($p = 0.06$). There were no lesions without nonperipheral washout in CK19 positive HCCs group and CK19 negative HCCs group. It is obvious that about 69%(35/51) of CK19 positive HCCs and 30% (47/156) of CK19 negative HCCs had nonperipheral washout.There was not any statistical difference with regard to signal intense (SI) on T1-weighted, T2-weighted and DWI images when comparing CK19 positive HCCs group to CK19 negative HCCs group (Table 3).

3.2.2. MR morphological characteristics

Significantly statistical difference could be found regarding to targetoid appearance between CK19 positive and negative HCCs groups ($p = 0.001$). Targetoid appearance was presented in 11 of 51 HCCs (21.6%) in the CK19 positive HCCs group and in 9 of 156 patients (5.8%) in CK19 negative HCCs group, respectively. In regard to gross morphology on MR imaging, there was a statistical difference between CK19 positive and negative groups ($p = 0.003$) and the majority of HCCs were round or oval. Round or oval HCC lesions was presented in 28 of 51 HCCs (54.9%) in the CK19 positive HCCs group and in 115 of 156 patients (73.7%) in CK19 negative HCCs group, respectively ($p = 0.004$). (Table 3, Figs. 2 and 3).

3.2.3. Uni/multivariate analyses for risk factors of CK19 positive/negative HCCs groups

To extract the factors associated with CK19 positive HCCs, we performed further analyses by univariate, as well as multivariate analyses. AFP > 20 ng/ml (OR = 5.1, $p < 0.0001$), rim APHE (OR = 4.1, $p < 0.0001$)and targetoid appearance (OR = 4.5, $p = 0.008$)were significant risk factors for CK19 positive HCCs by univariate analysis. Compared to CK19 positive HCCs group, nonperipheral "washout" (OR = 0.2, $p < 0.0001$)was more common in CK19 negative group. On

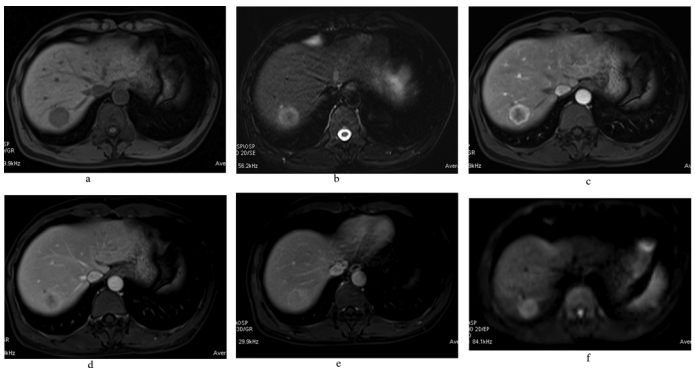

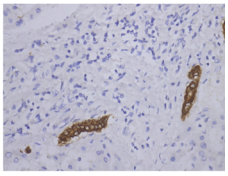

Fig. 2. Surgically confirmed hepatocellular carcinoma with CK19-positive in a 68-year-old man. The tumor showed hypointense on precontrast T_1-weighted imaging (2a),moderate hyperintense on T_2-weighted imaging (2b), progressive enhancement (2c-e), targetoid appearance (rim arterial phase enhancement (2c) and target-like on diffusion-weighted imaging at b = 500 s/mm^2 (2f)) and enhancing "capsule" on delay phase (2e). CK19 was positive on immunohistological examination (X200) (2 g).

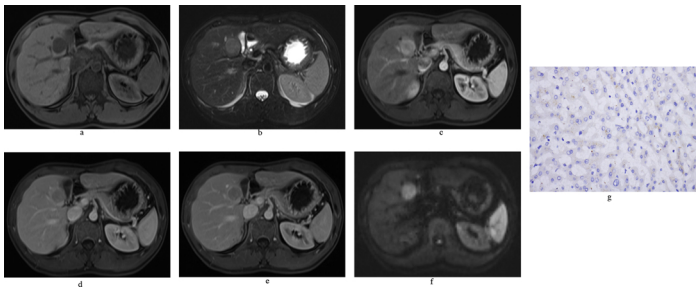

Fig. 3. Surgically confirmed hepatocellular carcinoma with CK19-negative in a 41-year-old woman. The tumor showed hypointense on precontrast T_1-weighted imaging (3a),moderate hyperintense on T_2-weighted imaging (3b), arterial phase hyper-enhancement with "washout" on portal venous phase and delay phase (3c-e), globally hyperintense on diffusion-weighted imaging at b = 500 s/mm^2 (3f)) and enhancing "capsule" on delay phase (3e). CK19 was negative on immunohistological examination(X200) (3 g).

multivariate analyses associated with CK19 positive HCCs group, AFP > 20 ng/ml (OR: 5.9, CI: 2.4–14.3, p < 0.0001) and targetoid appearance including targetoid dynamic enhancement(rim APHE,peripheral"washout", delayed central enhancement) and targetoid appearance on DWI.(OR: 4.2, CI:1.5–12.2, p = 0.022) were extracted as independent risk factors associated with CK19 positive HCCs group. (Table 4, Figs. 2,3).

4. Disscussion

Our study results demonstrated that absence of washout, targetoid appearance on DWI or contrast-enhanced images as well as elevated serum AFP were significant risk predictors for CK19-positive HCC, indicating that HCCs with CK19 expression do not meet classic diagnostic criteria for HCC but conform to imaging feature for LR-M lesions based on LI-RADS ver. 2017.

Previous studies had demonstrated that atypical MRI enhancement pattern often presented progressive or stable pattern of enhancement with respect to intrahepatic cholangiocarcinoma (ICC) [21,22]. However, Huang B et al [23] reported that 14.2% (87/612) small (≤ 3 cm) HCC showed progressive(3.9%) or displayed stable(10.3%) contrast enhancement at dynamic MR imaging, so they concluded that absence of contrast medium "washout" could be the enhancement pattern of small HCC. We identified that absence of "washout" was more common in CK19-positive HCCs group compared to CK19-negative group. CK19, a progenitor cell marker, was deemed to reflect HCC with biliary differentiation which can cause desmoplastic stroma within tumor [24]. And this biliary differentiation component may contribute to prolonged retention of contrast medium retention by abundant fibrosis of CK19-positive HCCs group. Meanwhile, HCC with biliary differentiation may result in the intermediate morphologic characteristics between HCC and ICC.

In the present study, targetoid appearance (rim APHE, peripheral "washout", delay central enhancement on dynamic contrast-enhanced MR imaging as well as a target sign on DWI) was verified as a valuable factor for predicting CK19-positive HCC. In previous study, rim APHE and/or target sign on the DWI were identified as significant and independent variable predictors of small ICC [25,26]. This is considered to be related to the pathological features of ICC with peripheral hyper-

Table 4
Univariate and Multivariate Analysis of risk factors for K19 positive hepatocellular carcinoma.

Variates	odds ratio (95% confidence interval)			
	Univariate Analysis	P-Value	Multivariate Analysis	P-Value
Sex	2.2(1.0,5.0)	0.064		
Age	1.0(0.96,1.02)	0.55		
Maximum diameter	1.0 (0.99,1.01)	0.837		
AFP > 20 ng/ml	5.1(2.3,11.6)	< **0.0001**	5.9(2.4, 14.3)	< **0.0001**
CEA > 5 ng/ml	2.2(0.8,5.8)	0.105		
CA-199 > 37U/ml	1.7(0.8,3.8)	0.205		
TB	1.0(0.96,1.02)	0.507		
Albumin	0.972(0.928,1.017)	0.220		
Platelet	1.001(0.997,1.006)	0.587		
HBV/HCV/ No*	1.2(0.6, 2.5)	0.639		
Portal vein embolization	0.8(0.2,2.8)	0.666		
MVI	1.5 (0.8,2. 9)	0.186		
Signal on T2WI	0.9(0.4,2.1)	0.778		
Signal on T1WI	68427202(0,∞)	0.999		
Signal on DWI images	0.3(0.1,1.8)	0.197		
rim APHE	4.1(2.1,8.0)	< **0.0001**		
Nonperipheral washout	0.2(0.1,0.4)	< **0.0001**	0.2(0.1, 0.4)	< **0.0001**
Hemorrhage	0.9(0.4,1. 8)	0.706		
Fat content	1. 2(0. 6,2.5)	0.648		
Capsule-like enhancement	1.4(1.0,1.9)	0.051		
Corona enhancement	3.1(0.4,22.9)	0.258		
Cholangiectasisc	2.1(0.3,12.8)	0.429		
Targetoid appearance	4.5(1.7,11.6)	**0.008**	4.2 (1. 5, 12.2)	**0.022**
Liver surface invasion	1.9(1.0,3.7)	0.057		
Tumor margin	0.7(0.3,1.4)	0.298		
MR gross morphology	1.3(1.0,1. 8)	0.077		

Note: AFP,alphafetoprotein;CA-199,carbohydrate antigen19-9;CEA,carcino embryonie antigen; TB, total bilirubin; HBV, hepatitis B varus; HCV, hepatitis C varus; MVI, microvascular invasion; DWI,diffusion weighted imaging; APHE: arterial phase hyperenhancement; MR,magnetic resonance.
No* stands for no HBV and HCV infection.

cellularity and central stromal fibrosis. HCC with biliary differentiation may be partly similar pathological characteristics of ICC. Furthermore, fibrous stroma formation is more frequent in CK19-positive HCC in comparison with conventional HCC [11].

In our study, we found that non-rim APHE could be regarded as a differential factor between CK19-positive and negative HCCs only in univariate analysis. Upon the hyper-enhancement of arterial phase, it is a pivotal criterion in the characterization of HCC based on LI-RADS [27]. Tumor growth is dependent on blood supply, which can be reflected by the degree of enhancement of tumor on dynamic contrast-enhanced MRI. In univariate analysis study, CK19-positive HCCs showed weaker enhancement on arterial phase than CK19-negative HCCs. The results were consistent with the findings from a previous study by Chung GE et al [18], which showed that CK19 was more frequently expressed in hypo-vascular HCC than in hyper-vascular tumors. We failed to demonstrate a significant benefit for enhancing "capsule" for differentiating CK19-positive from CK19-negative HCC. The reasons may be due to selection bias for relatively small size of a retrospective study. Moreover, CK19-positive HCC may partially keep inherent characteristics of conventional HCC.

AFP > 20 ng/ml was identified as an another independent risk factor associated with CK19 positive HCCs. AFP was one of the first protein tumor markers discovered [28]. And in patients with HCC, raised serum AFP plasma levels are positively associated with the status of poor cellular differentiation, microvascular invasion and tumor recurrence [29,30]. This is in keeping with the high aggressive of biologic behavior for CK19-positive HCC.

There are several limitations to our study. Firstly, selection bias could not be avoided due to the study performed retrospectively. In addition, there was inconformity among MR examinations which was conducted by using three different MR systems with different imaging parameters. Secondly, in our study we only focused on the analyses of MR morphological features based on LI-RADS ver.2017 routinely used in the clinical practice, and did not analyze quantitative measurements such as apparent diffusion coefficient value of DWI, which is subject to measure errors caused by technical variations among different MR scanners. Thirdly, targetoid sign was evaluated on DWI or dynamic enhanced MR imaging with an extracellular contrast agent. In our department, gadoxetic acid-enhanced MR imaging is not routinely used for abdominal MR imaging because of medical insurance, so we could not assess targetoid sign on transitional phase and hepatobiliary phase described in the LI-RADS ver.2017. Fourthly, non-HCC malignancies were not included in our study. Therefore, our study demonstrated which features are more commonly associated with CK19 positive HCC, but could not demonstrate that these factors can actually predict CK19 positive HCC in clinical practice, where the majority of lesions with targetoid appearance are ICC and combined HCC-CCA.

5. Clinical impact and conclusions

CK19 is a well-known marker for invasiveness of HCC and may be a novel therapeutic target for treatment of HCC [31–33]. Surgery or biopsy is invasive for the assessment of CK19 status in HCC patients. MRI including contrast-enhancement and DWI is a promising noninvasive alternative method that can be easily acquired in clinical practice. Our results suggested that MR features using LI-RADS ver.2017 especially LR-M criteria hold promise to identify CK19-positive from CK19-negative HCCs. Our study demonstrated that the targetoid features are more common in CK19-positive HCC, but as the study population did not include nonHCC malignancies, the conclusion cannot state that targetoid features are predictive of CK19-positive HCC. The current results should be further validated by prospective study with a large patient cohort.

Conflict of Interest

The authors of this manuscript declare no relationships with any companies, whose products or services may be related to the subject matter of the article.

Acknowledgements

This work was supported by the Key Program of Health and Family Planning Commission of Shanghai [grant number 201540383]. The authors of this manuscript declare no relationships with any companies, whose products or services may be related to the subject matter of the article.

References

[1] J. Ferlay, I. Soerjomataram, R. Dikshit, S. Eser, C. Mathers, M. Rebelo, et al., Cancer incidence and mortality worldwide: sources, methods and major patterns in GLOBOCAN 2012, Int. J. Cancer 136 (2015) E359–86.
[2] Lindsey A. Torre, Freddie Bray, Rebecca L. Siegel, Jacques Ferlay, Joannie Lortet-Tieulent, Ahmedin Jemal. Global Cancer statistics, 2012, CA Cancer J. Clin. 65 (2015) 87–108.
[3] W.T. London, K.A. McGlynn, Liver cancer, in: D. Schottenfeld, J. FraumeniJr (Eds.), Cancer Epidemiology and Prevention, 3rd ed., Oxford University Press, New York, 2006.
[4] T. Longerich, M.M. Mueller, K. Breuhahn, P. Schirmacher, A. Benner, C. Heiss, Oncogenetic tree modeling of human hepatocarcinogenesis, Int. J. Cancer 130 (2012) 575–583.
[5] A. Kitao, Y. Zen, O. Matsui, T. Gabata, Y. Nakanuma, hepatocarcinogenesis: multistep changes of drainage vessels at CT during arterial portography and hepatic arteriography—radiologic-pathologic correlation1, Radiology 252 (2009) 605–614.
[6] N.K. Mohamed, M.A. Hamad, M.Z. Hafez, K.L. Wooley, M. Elsabahy, Nanomedicine in management of hepatocellular carcinoma: challenges and Opportunities, Int. J. Cancer (2016), https://doi.org/10.1002/ijc.30517 [Epub ahead of print].
[7] R.H. Yuan, Y.M. Jeng, R.H. Hu, P.L. Lai, P.H. Lee, C.C. Cheng, et al., Role of p53 and β-catenin mutations in conjunction with CK19 expression on early tumor recurrence andprognosis of hepatocellular carcinoma, J. Gastrointest. Surg. 15 (2011) 321–329.
[8] L. Mishra, T. Banker, J. Murray, S. Byers, A. Thenappan, A.R. He, et al., Liver stem cells and hepatocellular carcinoma, Hepatology 49 (2009) 318–329.
[9] Z.S. Niu, X.J. Niu, M. Wang, Management of hepatocellular carcinoma: predictive value of immunohistochemical markers for postoperative survival, World J. Hepatol. 7 (2015) 7–27.
[10] O. Govaere, M. Komuta, J. Berkers, B. Spee, C. Janssen, F. de Luca, et al., Keratin 19: a key role player in the invasion of human hepatocellular carcinomas, Gut 63 (2014) 674–685.
[11] H. Kim, G.H. Choi, D.C. Na, E.Y. Ahn, G.I. Kim, J.E. Lee, et al., Human hepatocellular carcinomas with "stemness"-related marker expression: keratin 19 expression and a poor prognosis, Hepatology 54 (2011) 1707–1717.
[12] E.A. Pomfret, K. Washburn, C. Wald, M.A. Nalesnik, D. Douglas, M. Russo, et al., Report of a national conference on liver allocation in patients with hepatocellular carcinoma in the United States, Liver Transpl. 16 (3) (2010) 262–278.
[13] J. Bruix, M. Sherman, Management of hepatocellular carcinoma: an update, Hepatology 53 (2011) 1020–1022.
[14] A.Z. Kielar, V. Chernyak, M.R. Bashir, R.K. Do, K.J. Fowler, D.G. Mitchell, et al., LI-RADS 2017: an update, J. Magn. Reson. Imaging 47 (6) (2018) 1459–1474.
[15] K.M. Elsayes, J.C. Hooker, M.M. Agrons, A.Z. Kielar, A. Tang, et al., Version of LI-RADS for CT and MR imaging: an update, Radiographics 37 (7) (2017) 1994–2017 2017.
[16] S.Y. Choi, S.H. Kim, C.K. Park, J.H. Min, J.E. Lee, Y.H. Choi, et al., Imaging features of gadoxetic acid-enhanced and diffusion-weighted MR imaging for identifying cytokeratin 19-positive hepatocellular carcinoma: a retrospective observational study, Radiology 286 (3) (2018) 897–908.
[17] H.T. Jeong, M.J. Kim, Y.E. Kim, Y.N. Park, G.H. Choi, J.S. Choi, MRI features of hepatocellular carcinoma expressing progenitor cell markers, Liver Int. 32 (2012) 430–440.
[18] G.E. Chung, J.H. Lee, J.H. Yoon, S.J. Myung, K. Lee, J.J. Jang, et al., Prognostic implications of tumor vascularity and its relationship to cytokeratin 19 expression in patients with hepatocellular carcinoma, Abdom. Imaging 37 (2012) 439–446.
[19] X.X. Hu, Z.X. Yang, H.Y. Liang, Y. Ding, R. Grimm, C.X. Fu, et al., Whole-tumor MRI histogram analyses of hepatocellular carcinoma: correlations with Ki-67 labeling index, J. Magn. Reson. Imaging 46 (2) (2017) 383–392.
[20] W.T. Wang, L. Yang, Z.X. Yang, X.X. Hu, Y. Ding, X. Yan, et al., Assessment of microvascular invasion of hepatocellular carcinoma with diffusion kurtosis imaging, Radiology 286 (2) (2018) 571–580.
[21] Jordi Rimola, Alejandro Forner, Maria Reig, Ramon Vilana, Carlos Rodrı′guez de Lope, Carmen Ayuso, et al., Cholangiocarcinoma in cirrhosis: absence of contrast washout in delayed phases by magnetic resonance imaging avoids misdiagnosis of hepatocellular carcinoma, Hepatology 50 (2009) 791–798.
[22] R. Kim, J.M. Lee, C.I. Shin, E.S. Lee, J.H. Yoon, I. Joo, et al., Differentiation of intrahepatic mass-forming cholangiocarcinoma from hepatocellular carcinoma on gadoxetic acid-enhanced liver MR imaging, Eur. Radiol. 26 (6) (2016) 1808–1817.
[23] B. Huang, L. Wu, X.Y. Lu, F. Xu, C.F. Liu, W.F. Shen, Small intrahepatic cholangiocarcinoma and hepatocellular carcinoma in cirrhotic livers may share similar enhancement patterns at multiphase dynamic MR imaging, Radiology 281 (2016) 150–157.
[24] S. Aishima, Y. Nishihara, Y. Kuroda, K. Taguchi, T. Iguchi, A. Taketomi, et al., Histologic characteristics and prognostic significance in small hepatocellular carcinoma with biliary differentiation, Am. J. Surg. Pathol. 31 (2007) 783–791.

[25] T. Ni, X.S. Shang, W.T. Wang, X.X. Hu, M.S. Zeng, S.X. Rao, Different MR features for differentiation of intrahepatic mass-forming cholangiocarcinoma from hepatocellular carcinoma according to tumor size, Br. J. Radiol. 5 (June) (2018) 20180017, , https://doi.org/10.1259/bjr.20180017.
[26] Hyun Jeong Park, Young Kon Kim, Min Jung Park, Won Jae Lee, Small intrahepatic mass-forming cholangiocarcinoma: target sign on diffusion-weighted imaging for differentiation from hepatocellular carcinoma, Abdom. Imaging 38 (2013) 793–801.
[27] I. Cruite, A. Tang, C.B. Sirlin, Imaging-based diagnostic systems for hepatocellular carcinoma, AJR Am. J. Roentgenol. 201 (2013) 41–55.
[28] C. Sauzay, A. Petit, A.M. Bourgeois, J.C. Barbare, B. Chauffert, A. Galmiche, et al., Alpha-foetoprotein (AFP): a multi-purpose marker in hepatocellular carcinoma, Clin. Chim. Acta 463 (2016) 39–44.
[29] W.J. Ma, H.Y. Wang, L.S. Teng, Correlation analysis of preoperative serum alpha-fetoprotein (AFP) level and prognosis of hepatocellular carcinoma (HCC) after hepatectomy, World J. Surg. Oncol. 11 (212) (2013).
[30] M. Meguro, T. Mizuguchi, T. Nishidate, K. Okita, M. Ishii, S. Ota, et al., Prognostic roles of preoperative α-fetoprotein and des-γ-carboxy prothrombin in hepatocellular carcinoma patients, World J. Gastroenterol. 21 (2015) 4933–4945.
[31] T. Kawai, K. Yasuchika, T. Ishii, H. Katayama, E.Y. Yoshitoshi, S. Ogiso, et al., Keratin 19, a Cancer stem cell marker in human hepatocellular carcinoma, Clin. Cancer Res. 21 (2015) 3081–3091.
[32] T. Kawai, K. Yasuchika, T. Ishii, H. Katayama, E.Y. Yoshitoshi, S. Ogiso, et al., Identification of keratin 19-positive cancer stem cells associating human hepatocellular carcinoma using CYFRA 21-1, Cancer Med. 6 (2017) 2531–2540.
[33] M. Takano, K. Shimada, T. Fujii, K. Morita, M. Takeda, Y. Nakajima, et al., Keratin 19 as a key molecule in progression of human hepatocellular carcinomas through invasion and angiogenesis, BMC Cancer 16 (2016) 903.